Original Article

Diagnostic performance of contrast-enhanced ultrasound in breast lesions: what diagnostic models could be used for lesions of different sizes?

Naiqin Fu[1], Junkang Li[1,2], Bo Wang[1], Ying Jiang[1], Shiyu Li[1], Ruilan Niu[1], Zhili Wang[1]

[1]Department of Ultrasound, The First Medical Center, Chinese PLA General Hospital, Beijing, China; [2]Department of Ultrasound, Chinese PLA 63820 Hospital, Mianyang, China

Contributions: (I) Conception and design: N Fu, J Li, Z Wang; (II) Administrative support: B Wang, Z Wang; (III) Provision of study materials or patients: R Niu, Y Jiang, S Li; (IV) Collection and assembly of data: N Fu, J Li, R Niu; (V) Data analysis and interpretation: N Fu, B Wang, S Li, J Li; (VI) Manuscript writing: All authors; (VII) Final approval of manuscript: All authors.

Correspondence to: Zhili Wang, MD. Department of Ultrasound, The First Medical Center, Chinese PLA General Hospital, 28 Fuxing Road, Beijing 100853, China. Email: wzllg@sina.com.

Background: Previous studies show the size of lesions could affect the diagnostic accuracy of contrast-enhanced ultrasound (CEUS). It is unclear whether CEUS has good diagnostic performance for lesions ≤2.0 and ≤1.0 cm. It is beneficial for the early diagnosis to explore the application of CEUS in breast lesions of different sizes. This study aims to analyze the diagnostic performance of CEUS and explore diagnostic models better suited to breast lesions of different sizes.

Methods: A total of 1,059 lesions (656 benign and 403 malignant) examined by ultrasound and CEUS with definite pathological results were included in this retrospective study and divided into training (n=847) and validation (n=212) sets. All lesions were divided into three groups according to size. Diagnostic models (M_0: all lesions; M_1: ≤1.0 cm, M_2: >1.0–2.0 cm, and M_3: >2.0 cm) were developed through logistic regression analyses of CEUS features from the training set. Diagnostic performance was evaluated using the area under the receiver operating characteristic curve (AUC) and validated in the validation set.

Results: The median age of patients was 45±11 years (range, 18–80 years). The AUC values of M_0 combined with the Breast Imaging Reporting and Data System (BI-RADS) in the training and validation sets were 0.921 and 0.922, respectively (P=0.893). The AUC values of M_0 combined with BI-RADS in the three groups were 0.844, 0.936 and 0.928 respectively. M_0 was less effective in diagnosing lesions ≤1.0 cm (0.844 *vs.* 0.921, P=0.029). The AUC of M_1 combined with BI-RADS for lesions ≤1.0 cm was higher than that of M_0 (0.893 *vs.* 0.844, P=0.047), and M_2 and M_3 had no statistical difference in diagnostic performance when compared with M_0 (P=0.243; P=0.246).

Conclusions: The diagnostic performance of CEUS was closely related to lesion size. Establishing a new diagnostic model for lesions ≤1.0 cm can improve the CEUS diagnostic performance for breast lesions ≤1.0 cm.

Keywords: Breast cancer; ultrasound (US); contrast-enhanced ultrasound (CEUS); size

Submitted May 25, 2023. Accepted for publication Nov 17, 2023. Published online Dec 22, 2023.
doi: 10.21037/gs-23-223
View this article at: https://dx.doi.org/10.21037/gs-23-223

Introduction

Ultrasound (US) is widely used for breast check-up due to its wide availability, low price, and patient acceptance. In addition to conventional US, the development of contrast-enhanced ultrasound (CEUS) allows evaluation of microvascular structures, density, and blood perfusion of tumors, offering more valuable information about lesions (1). Previous studies have confirmed the value of CEUS in the diagnosis of benign and malignant breast lesions (2-4). However, there are some limitations in applying CEUS to the breast and there is a lack of uniform diagnostic criteria. In a previous study, size of lesions was shown to affect the diagnostic accuracy of CEUS. The diagnostic value of CEUS varied with the size of lesions and it had a higher accuracy for lesions >2.0 cm (5). Tumor angiogenesis varies with tumor size (6). In addition, tumor size is considered an important reference point for breast cancer treatment, as well as a strong predictor of prognosis (7). However, it is unclear whether CEUS has good diagnostic performance for lesions ≤1.0 and ≤2.0 cm. For early diagnosis, it is beneficial to explore the application of CEUS in breast lesions of different sizes. In this study, the lesions were divided into three groups according to their size to analyze the diagnostic performance of CEUS in breast lesions of different sizes and to explore more models better applied to these lesions. We present this article in accordance with the STARD reporting checklist (available at https://gs.amegroups.com/article/view/10.21037/gs-23-223/rc).

Highlight box

Key findings

- The diagnostic efficiencies of contrast-enhanced ultrasound (CEUS) for lesions of different sizes varied.
- New models were established for lesions of different sizes.
- Diagnostic model for lesions ≤1.0 cm was different from that for other lesions.

What is known and what is new?

- The diagnostic value of CEUS had a higher accuracy for lesions >2.0 cm.
- Diagnostic model for lesions ≤1.0 cm was different from that for other lesions.

What is the implication, and what should change now?

- CEUS is effective for the diagnosis of small breast lesions and different models are required for breast lesions of different sizes.

Methods

Patients selected

This study was conducted in accordance with the Declaration of Helsinki (as revised in 2013). This retrospective clinical diagnostic study was approved by the Ethics Committee of the Chinese PLA General Hospital (No. S2021-683-01). Informed consent was waived because of the retrospective nature of the study. The outcome of interest in this study was binary diagnosis of benign and malignant lesions. Between January 2021 and April 2022, 1,059 breast lesions from 1,059 consecutive patients who underwent US and CEUS at the General Hospital of the People's Liberation Army of China were retrospectively examined in this study. The inclusion criteria were as follows: (I) patients with newly found solid breast lesions; (II) patients with breast lesions examined by both US and CEUS successively; and (III) patients with definite pathological findings. The exclusion criteria were as follows: (I) patients who received radiotherapy and chemotherapy; (II) patients with a history of breast surgery; (III) incomplete or unable to accurately analyze the image information. The flowchart of patient selection is shown in *Figure 1*. Using histopathological results of the surgical or vacuum-assisted excisional specimens as the diagnostic standard, 654 malignant and 405 benign lesions were identified. These lesions were divided into three groups according to size (Group 1: ≤1.0 cm; Group 2: >1.0–2.0 cm, Group 3: >2.0 cm).

US equipment

All sonographic examinations were performed by ACUSON S2000 US system (Siemens, Erlangen, Germany) with a 9L4 linear array probe. The contrast agent used for CEUS imaging was SonoVue (Bracco International, Milan, Italy), a sterile freeze-dried powder consisting of phospholipid microbubbles, which can be metabolized through respiration within 30 min.

US examination

Both conventional US and CEUS examinations were performed by two physicians with more than 5 years of experience in breast ultrasonography. Once a lesion was detected, its images obtained in different planes were stored and its size was recorded. The size was defined as the

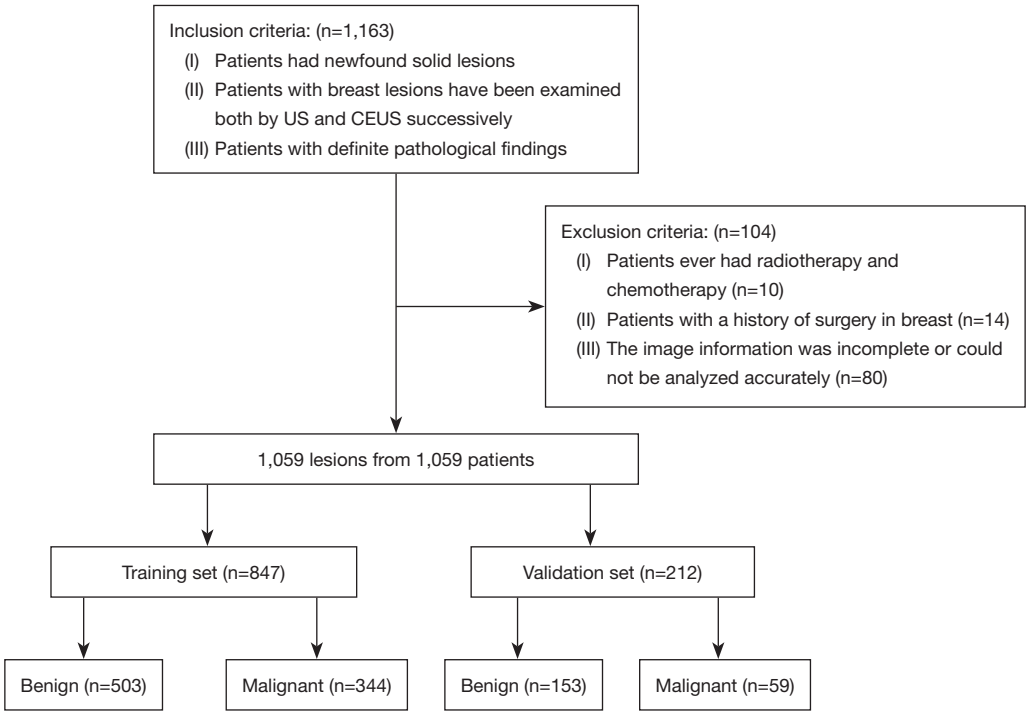

Figure 1 Flowchart of the selection of patients. US, ultrasound; CEUS, contrast-enhancement US.

greatest dimension of tumor measured using conventional US. If a patient had multiple lesions, the one with the largest diameter was included in this study. Subsequently, the system was switched to CEUS mode, and the mechanical index was set as 0.06–0.08. The optimal plane for CEUS showed both the largest diameter and sufficient surrounding normal tissue. A bolus of 5.0 mL of contrast agent was injected into an antecubital vein, followed by a flush of 5.0–10.0 mL of saline. Applying dual-screen mode, conventional US and CEUS images of the same plane were displayed in real time for observation and comparison. The lesion and surrounding tissues were recorded as real time images and a 3-min-lasting video for follow-up analyses. If the same patient required reexamined by CEUS, the interval was >20 min.

US and CEUS image analyses

All conventional US and CEUS images were analyzed independently by two physicians blinded to clinical information and final pathological results. Final decisions were made by consensus. According to the American College of Radiology Breast Imaging Reporting and Data System (BI-RADS) (8), lesions examined using conventional US were divided into five categories: 3, 4A, 4B, 4C, and 5.

According to CEUS performance, all lesions were evaluated for the following features:

(I) Enhancement direction (centripetal or centrifugal/diffuse/absent).
(II) Enhancement degree: enhanced intensity compared with surrounding breast tissue (hyper-/iso-/nonenhancement or hypo-enhancement).
(III) Enhancement homogeneity: internal homogeneity of the lesion at the peak of enhancement (homogeneous or heterogeneous).
(IV) Blood perfusion defects: the area without microbubble contrast media perfusion (present or absent).
(V) Enhancement scope: comparison of the maximum diameter in CEUS images with two-dimensional images (enlarged or not enlarged).
(VI) Radial or penetrating vessels: radial enhancement around the lesion (present or absent).
(VII) Enhancement shape (regular or irregular).
(VIII) Wash-in time: entered time compared with surrounding breast tissue (earlier or synchronous/

Table 1 Clinical and histological results of all cases

Variables	Training set	Validation set
Age (years), mean ± standard deviation	45±11	45±12
Lesion size (cm), mean ± standard deviation	1.9±1.3	1.5±0.9
Histological benign, n (%)	n=503	n=153
Fibroadenoma	238 (47.3)	49 (32.0)
Mastopathy	214 (42.5)	61 (39.9)
Intraductal papilloma	25 (5.0)	31 (20.3)
Benign phyllodes tumor	4 (0.8)	1 (0.7)
Hamartoma	1 (0.2)	0
Inflammation	21 (4.2)	11 (7.2)
Histological malignant, n (%)	n=344	n=59
Invasive carcinoma of no special type	293 (85.2)	42 (71.2)
Invasive lobular carcinoma	6 (1.7)	0
Ductal carcinoma *in situ*	37 (10.8)	14 (23.7)
Mucinous carcinoma	5 (1.5)	1 (1.7)
Lobular carcinoma *in situ*	1 (0.3)	1 (1.7)
Medullary carcinoma	1 (0.3)	1 (1.7)
Diffuse large B-cell lymphoma	1 (0.3)	0

later/absent).

(IX) Wash-out time: withdrew time compared with surrounding breast tissue (earlier/synchronous/absent or later).

When the enhancement degree of a lesion was non-enhancement, the enhancement direction, wash-in time, and wash-out time of the lesion were defined as absence.

Sample size calculation

The sample size was calculated on the basis of literature review (5). The sensitivity and specificity of CEUS for breast lesions were 0.76 and 0.86, respectively. The power (1-β) was 0.90, and allowed error was 0.1. Considering the loss of follow-up rate of 10%, the study should include 546 benign and 219 malignant lesions, for a total of 765 cases.

Statistical analysis

Statistical analyses were performed using SPSS 25.0 (SPSS Inc, Chicago, IL, USA) MedCalc 20 (MedCalc Software Ltd, Ostend, Belgium) and PASS 15.0 (PASS Software, Rijswijk, The Netherlands). Patients who underwent US and CEUS between January 2021 and December 2021 were included in the training set, and patients who underwent US and CEUS between January 2022 and April 2022 were included in the validation set. Independent *t*-test was used for normally distributed data, whereas Mann-Whitney *U* test was used for non-normally distributed data. Diagnostic models were established using multivariate binary logistic regression analyses of CEUS features from the training set. Diagnostic performance was evaluated using the area under the receiver operating characteristic curve (AUC) and validated in the validation set. When combining diagnostic models and BI-RADS, if the CEUS model result was positive, the original BI-RADS score was raised one level. If negative, the original BI-RADS score was downgraded one level. After the receiver operating characteristic (ROC) curve was operated, AUC values were calculated, and Youden's index was used to calculate the optimal cutoff values. The cutoff value divided the samples into positive and negative, and then sensitivity and specificity were calculated. The DeLong test was used to compare the ROC curves. Two-sided P values of <0.05 were considered indicative of statistically significant differences.

Results

Basic information of patients and lesions

All 1,059 patients were women aged 18–80 years, with a mean age of 45±11 years. All lesions had a mean size of 1.8±1.2 cm (range, 0.2–13.9 cm). A total of 847 lesions (80.0%) were included in the training set, and 212 (20.0%) were included in the validation set. Patient age, lesion size, and pathological types of training and validation sets are listed in *Table 1*. All lesions in the training set were divided into three groups. Groups 1 (*Figure 2*), 2 (*Figure 3*), and 3 (*Figure 4*) with 208, 362, and 277 lesions, respectively. No severe adverse events were reported during conventional US and CEUS examinations.

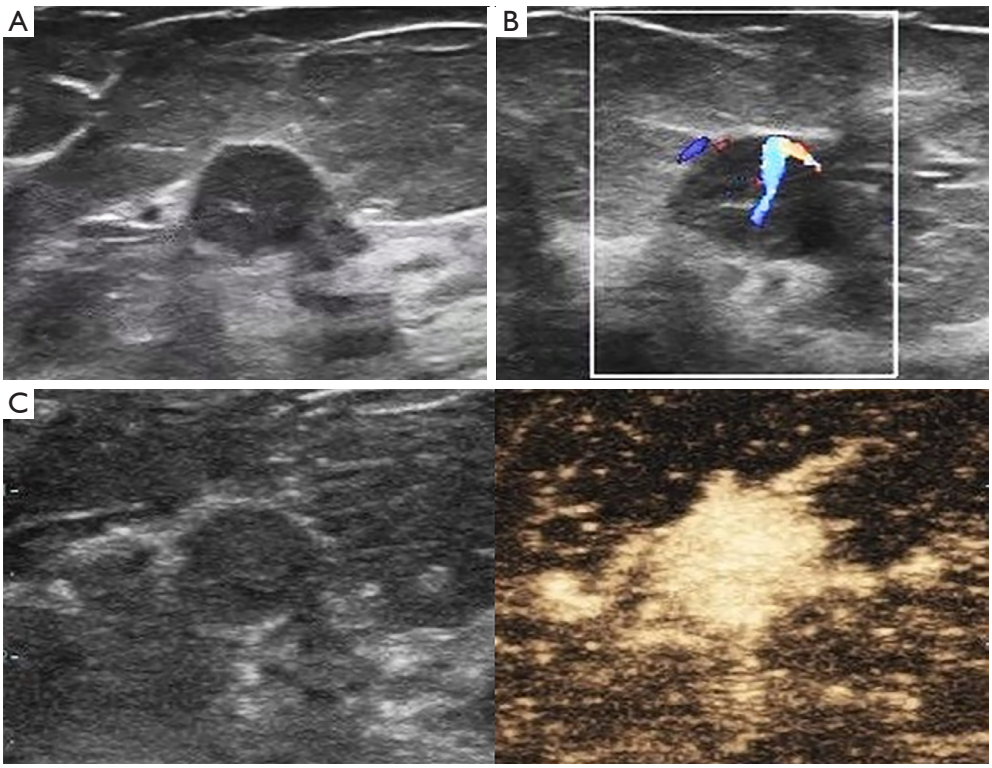

Figure 2 Images of a lesion with a size of 0.9 cm in a 73-year-old woman. (A,B) Conventional ultrasound shows an oval hypoechoic lesion with circumscribed margin and present vascularity. (C) Contrast-enhanced ultrasound shows that the lesion has homogeneous hyperenhancement, an enlarged enhancement scope, and radial or penetrating vessels. Histopathology reveals ductal carcinoma *in situ*.

Logistic regression analyses of CEUS features of all lesions

The BI-RADS categories of the 847 lesions in the training set, based on conventional US are shown in *Table 2*. The sensitivity, specificity, accuracy and AUC of BI-RADS categories were 83.7%, 81.2%, 82.2% and 0.875, respectively.

Univariate and multivariate regression analyses of CEUS features of all lesions in the training set are shown in *Table 3*. In univariate analysis, centripetal enhancement (P<0.001), hyperenhancement (P<0.001), heterogeneous enhancement (P<0.001), presence of blood perfusion defects (P<0.001), enlarged enhancement scope (P<0.001), presence of radial or penetrating vessels (P<0.001), irregular enhancement shape (P<0.001), ill-defined enhancement margin (P<0.001), earlier wash-in time (P<0.001) and later wash-out time (P<0.001) were associated with malignancy. All the aforementioned characteristics were subsumed in multivariate regression analysis. It showed that enhancement direction [odds ratio (OR) =2.31, P=0.001], blood perfusion defects (OR =1.72, P=0.028), scope (OR =5.45, P<0.001), radial or penetrating vessels (OR =2.30, P=0.001), shape (OR =1.96, P=0.031) and wash-out time (OR =1.94, P=0.003) were the independent influencing factors for malignant breast lesions.

M_0: the fitting model of all lesions is as follows.

$$\begin{aligned}\text{Logit}(P) = &-2.952 + 0.831X_1 + 0.571X_2 + 0.939X_3 \\ &+ 1.736X_4 + 0.857X_5 + 0.646X_6\end{aligned} \quad [1]$$

X_1 indicates enhancement direction (centrifugal/diffuse/absent, 0; centripetal, 1). X_2 indicates blood perfusion defects (iso/hypo/non-enhancement, 0; hyper-enhancement, 1). X_3 indicates enhancement shape (regular, 0; irregular, 1). X_4 indicates enhancement scope (not enlarged, 0; enlarged, 1). X_5 indicates radial or penetrating vessels (absent, 0; present, 1). X_6 indicates wash-out time (earlier/synchronous/absent, 0; later, 1).

In the training set, the sensitivity, specificity, accuracy, and AUC of the M_0 combined with BI-RADS were 84.8%, 85.7%, 85.3%, and 0.921 respectively. The AUC value of

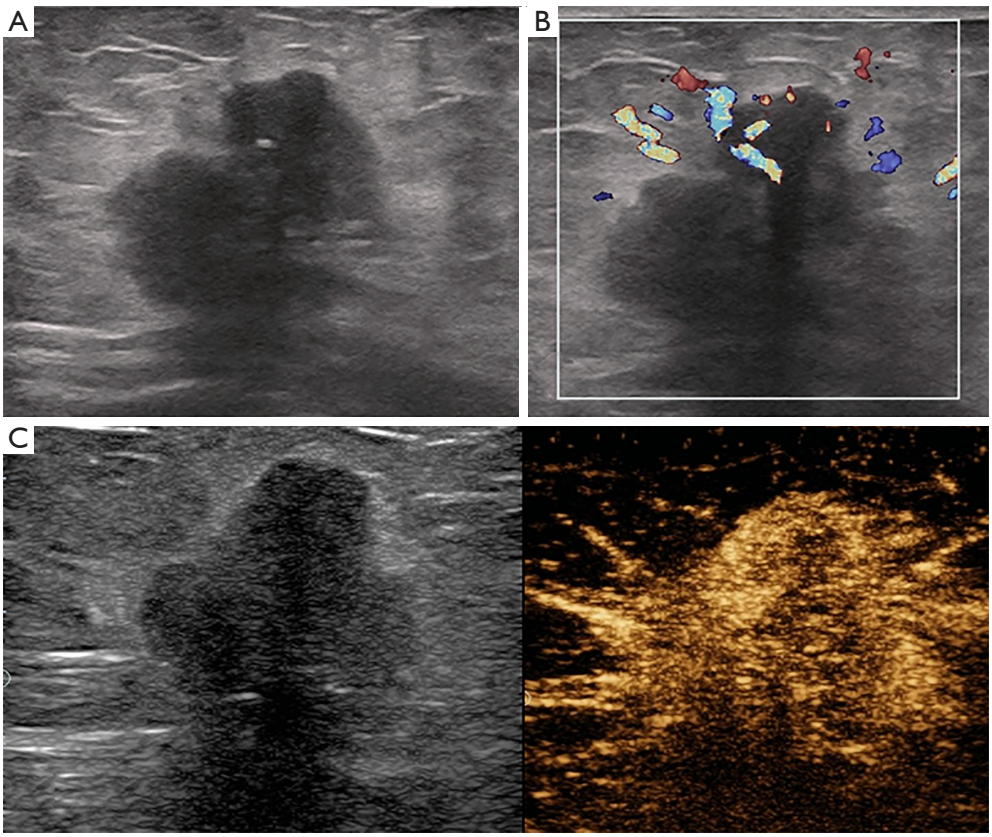

Figure 3 Images of a lesion with a size of 1.5 cm in a 75-year-old woman. (A,B) Conventional ultrasound shows an irregular hypoechoic lesion with an indistinct margin, shadowing posterior feature, and present vascularity. (C) Contrast-enhanced ultrasound shows that the lesion has heterogeneous hyperenhancement, an enlarged enhancement scope, and radial or penetrating vessels. Histopathology reveals invasive carcinoma.

M_0 combined with BI-RADS in the validation set was 0.922. No statistical differences were found between the training and validation sets (0.921 *vs.* 0.922, P=0.893), indicating that M_0 effectively diagnosed benign and malignant breast lesions in both datasets.

Comparison of the diagnostic performance of CEUS in three groups

M_0 was highly efficient when applied in Groups 2 and 3, while it was far inferior in Group 1. By applying M_0 into three groups and combining it with BI-RADS, the AUC values of three groups were 0.844, 0.936 and 0.928, respectively. M_0 was less effective in Group 1 (0.844 *vs.* 0.921, P=0.029), but fitted well in Groups 2 and 3 (0.936 *vs.* 0.921, P=0.360; 0.928 *vs.* 0.921, P=0.711). More details are presented in *Table 4* and the ROC curves of M_0 applying for three groups are shown in *Figure 5*.

Logistic regression analyses of CEUS features of lesions with different sizes

Univariate and multivariate analyses of Groups 1–3 are subsumed in *Figure 6* and detailed in Tables S1-S3.

In Group 1, there were statistically significant differences in enhancement direction (P=0.001), degree (P<0.001), scope (P<0.001), radial or penetrating vessels (P<0.001), shape (P<0.001), margin (P<0.001) and wash-in time (P<0.001) between benign and malignant lesions. All the above characteristics were subsumed in multivariate analysis, showing that scope was the independent influencing factor for malignant breast lesions (OR =2.710, P=0.001).

M_1: the fitting model of group 1 is as follows:

$$\begin{aligned}\text{Logit}(P) = &-2.427 + 0.116X_1 + 1.192X_2 - 0.877X_3 \\ &+ 1.114X_4 + 0.518X_5 + 2.096X_6 - 0.666X_7\end{aligned} \quad [2]$$

X_1 indicates direction (centrifugal/diffuse/absent, 0;

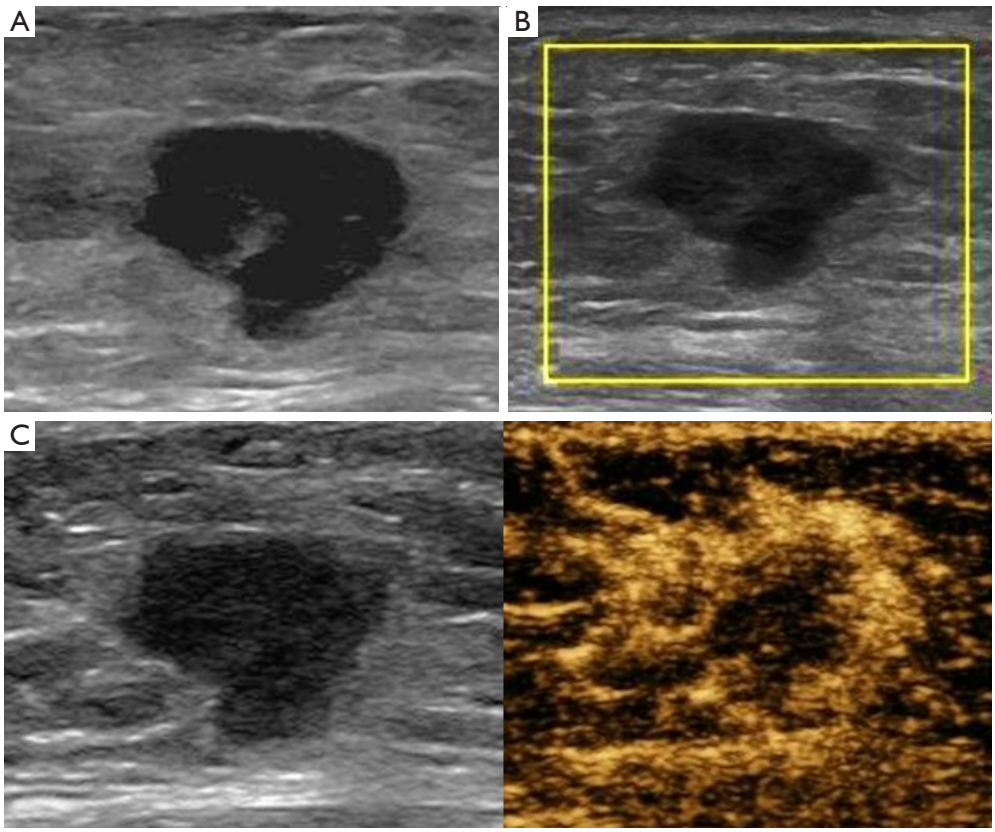

Figure 4 Images of a lesion with a size of 2.3 cm in a 40-year-old woman. (A,B) Conventional ultrasound shows an irregular hypoechoic lesion with an indistinct margin and absent vascularity. (C) Contrast-enhanced ultrasound shows that the lesion has heterogeneous hyperenhancement, an ill-defined margin, an irregular shape, an enlarged enhancement scope, perfusion defect, and radial or penetrating vessels. Histopathology reveals invasive carcinoma.

Table 2 BI-RADS categories of lesions from the training set

BI-RADS category	Final pathologic results		Total
	Benign (n=503)	Malignant (n=344)	
Category 3	108	3	111
Category 4A	300	53	353
Category 4B	79	117	196
Category 4C	15	95	110
Category 5	1	76	77
Total	503	347	847

BI-RADS, Breast Imaging Reporting and Data System.

centripetal, 1). X_2 indicates wash-in time (synchronous/later/absent, 0; earlier, 1). X_3 indicates degree (iso/hypo/non-enhancement, 0; hyper-enhancement, 1). X_4 indicates shape (regular, 0; irregular = 1). X_5 indicates margin (well-defined, 0; ill-defined, 1). X_6 indicates scope (not enlarged, 0; enlarged, 1). X_7 indicates radial or penetrating vessels (absent, 0; present = 1).

In the training set, the sensitivity, specificity, accuracy, and AUC of M_1 combined with BI-RADS were 89.1%, 79.1%, 81.5% and 0.893 respectively. The AUC of M_1 combined with BI-RADS in the validation set was 0.837. No statistical differences were noted between the training and validation sets (0.893 *vs.* 0.837, P=0.204), indicating that M_1 was effective in diagnosing benign and malignant breast lesions ≤1.0 cm in both datasets. The diagnostic efficiency of M_1 combined with BI-RADS was higher than that of M_0 combined with BI-RADS (0.893 *vs.* 0.844, P=0.047) (*Figure 7*).

In the same way, M_1 was established by Group 1, and so were the new models of Groups 2 and 3 performed. No statistical differences were noted between the diagnostic efficacy of the new models combined with BI-RADS

Table 3 Univariate and multivariate regression analysis of CEUS features of all lesions

CEUS features	Overall, n (%)		Univariate analysis		Multivariate analysis	
	Benign (n=503)	Malignant (n=344)	OR (95% CI)	P value	OR (95% CI)	P value
Enhancement direction						
Centrifugal/diffuse/absent	229 (45.5)	42 (12.2)	1 (reference)			
Centripetal	274 (54.5)	302 (87.8)	6.01 (4.16–8.67)	<0.001*	2.31 (1.42–3.76)	0.001*
Enhancement degree						
Iso/hypo/non-enhancement	271 (53.9)	47 (13.7)	1 (reference)			
Hyperenhancement	232 (46.1)	297 (86.3)	7.38 (5.18–10.51)	<0.001*	1.02 (0.48–2.14)	0.957
Enhancement homogeneity						
Homogeneous	194 (38.6)	75 (21.8)	1 (reference)			
Heterogeneous	309 (61.4)	269 (78.2)	2.25 (1.64–3.07)	<0.001*	1.11 (0.69–1.78)	0.659
Blood perfusion defects						
Absent	433 (86.1)	233 (67.7)	1 (reference)			
Present	70 (13.9)	111 (32.3)	2.94 (2.10–4.13)	<0.001*	1.72 (1.06–2.79)	0.028*
Enhancement scope						
Not enlarged	428 (85.1)	75 (21.8)	1 (reference)			
Enlarged	75 (14.9)	269 (78.2)	20.46 (14.35–29.17)	<0.001*	5.45 (3.36–8.83)	<0.001*
Radial/penetrating vessels						
Absent	466 (92.6)	168 (48.8)	1 (reference)			
Present	37 (7.4)	176 (51.2)	13.19 (8.88–19.60)	<0.001*	2.30 (1.39–3.81)	0.001*
Enhancement shape						
Regular	410 (81.5)	85 (24.7)	1 (reference)			
Irregular	93 (18.5)	259 (75.3)	13.43 (9.63–18.73)	<0.001*	1.96 (1.06–3.62)	0.031*
Enhancement margin						
Well-defined	392 (77.9)	105 (30.5)	1 (reference)			
Ill-defined	111 (22.1)	239 (69.5)	8.03 (5.88–10.97)	<0.001*	1.42 (0.79–2.54)	0.238
Wash-in time						
Synchronous/later/absent	284 (56.5)	53 (15.4)	1 (reference)			
Earlier	219 (43.5)	291 (84.6)	7.12 (5.05–10.02)	<0.001*	1.00 (0.47–2.10)	0.998
Wash-out time						
Earlier/synchronous/absent	311 (61.8)	67 (19.5)	1 (reference)			
Later	192 (38.2)	277 (80.5)	6.69 (4.85–9.23)	<0.001*	1.94 (1.25–3.01)	0.003*

*, statistical significance. CEUS, contrast-enhancement ultrasound; OR, odds ratio; CI, confidence interval.

Table 4 Comparison of diagnostic performance of M_0 in different groups

Group	Sensitivity (%)	Specificity (%)	Accuracy (%)	AUC	
				Value	P value
Total (n=847)					0.001*
BI-RADS	83.7	81.2	82.2	0.875	
CEUS	88.9	79.3	83.3	0.885	
Combined	84.8	85.7	85.3	0.921	
≤1.0 cm (n=208)					0.004*
BI-RADS	60.9	85.1	79.4	0.752	
CEUS	76.1	85.8	83.5	0.796	
Combined	84.8	82.4	83.0	0.844	
>1.0–2.0 cm (n=362)					<0.001*
BI-RADS	82.6	82.3	82.4	0.878	
CEUS	84.8	86.4	85.8	0.901	
Combined	92.8	81.4	85.8	0.936	
>2.0 cm (n=277)					0.007*
BI-RADS	91.2	73.9	84.0	0.899	
CEUS	84.9	79.1	82.5	0.883	
Combined	86.2	86.1	86.2	0.928	

*, statistical significance. AUC, area under the curve; BI-RADS, Breast Imaging Reporting and Data System; CEUS, contrast-enhancement ultrasound.

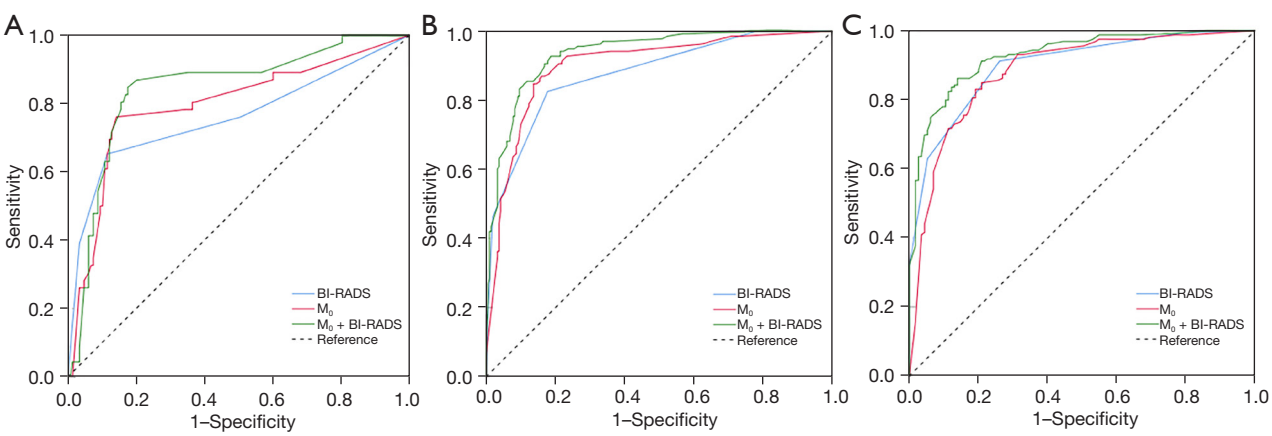

Figure 5 ROC curves for the fitting model (M_0) applied to three groups. (A) ROC curves for M_0, BI-RADS and their combination in Group 1. (B) ROC curves for M_0, BI-RADS and their combination in Group 2. (C) ROC curves for M_0, BI-RADS and their combination in Group 3. BI-RADS, Breast Imaging Reporting and Data System; ROC, receiver operating characteristic.

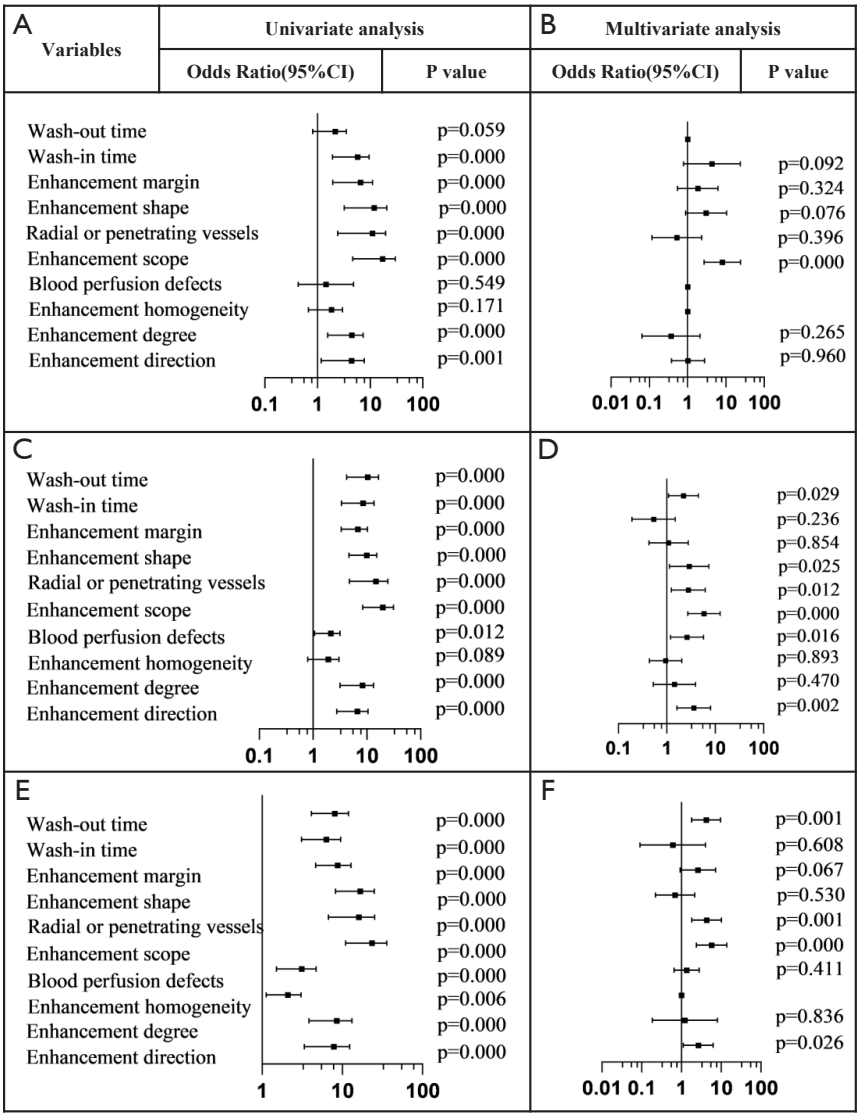

Figure 6 Forest plots summarizing univariate and multivariate regression of three Groups. (A,B) Forest plots for univariate and multivariate regression in Group 1. (C,D) Forest plots for univariate and multivariate regression in Group 2. (E,F) Forest plots for univariate and multivariate regression in Group 3. CI, confidence interval.

established by Groups 2 and 3 and that of M_0 combined with BI-RADS (0.937 *vs.* 0.936, P=0.243 and 0.934 *vs.* 0.928, P=0.246) (*Figure* 7).

Discussion

The diagnostic performance of CEUS varies for lesions of different sizes. Correct identification of these differences is vital for the diagnosis of breast lesions. Multivariate regression analysis showed that enhancement direction, wash-in time, degree, shape, margin, scope, and radial or penetrating vessels were independent factors associated with benign and malignant pathological results. A previous study had reported similar findings. Wan *et al.* (9) showed that enhancement degree, direction, homogeneity, margin, and radial or penetrating vessels could effectively distinguish between benign and malignant breast lesions.

During CEUS, the inflammatory response and the angiogenesis of malignant lesions are likely to cause enlarged enhancement scope, ill-defined margin and

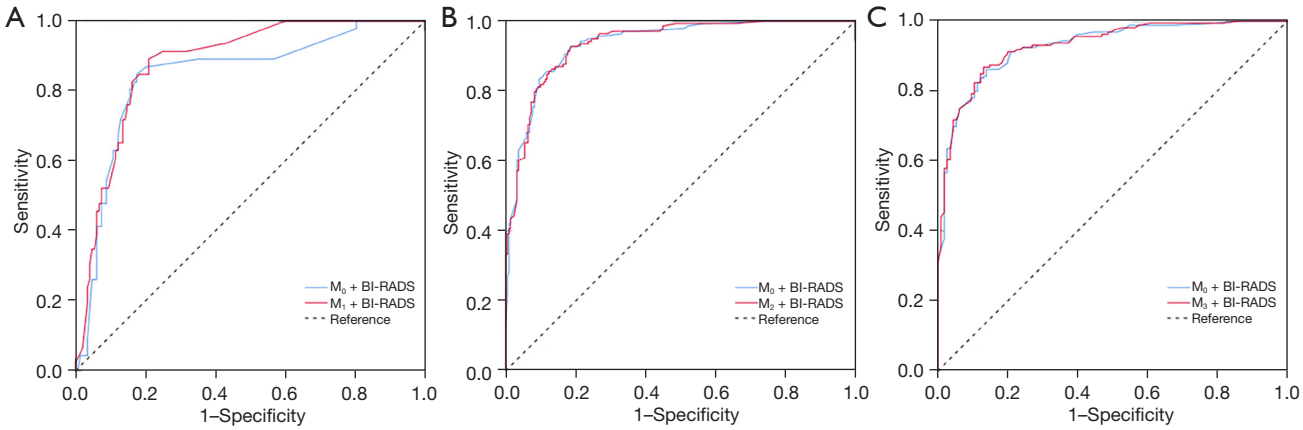

Figure 7 ROC curves comparing the fitting model (M_0) with new models established by three groups. (A) ROC curves comparing M_0 with M_1 established by Group 1. (B) ROC curves comparing M_0 with new model established by Group 2. (C) ROC curves comparing M_0 with new model established by Group 3. BI-RADS, Breast Imaging Reporting and Data System; ROC, receiver operating characteristic.

irregular shape, which play important roles in the diagnosis of benign and malignant breast lesions (10). Some studies showed that malignant tumors trigger local inflammatory responses that establish a primordial microenvironment (11,12). Tumor cells infiltrate cleavage products into surrounding normal tissues with the assistance of proteolytic enzymes and matrix degrading enzymes, stimulating angiogenesis in the surrounding area (13). More centripetal enhancement is observed in malignant lesions, whereas more centrifugal or diffuse enhancement is observed in benign ones. The direction of enhancement is related to tumor microvascular density (MVD) (14). In malignant tumors, the proportion of microvessels in peripheral region is higher than that in the central region, whereas in benign lesions, only slight differences are observed in the distribution (15,16). The blood perfusion defect is because of the fact that malignant lesions grow faster than benign ones, and local areas of the tumor are prone to necrosis with the increase in tumor volume, which is manifested as local blood perfusion defects during enhanced angiography (17,18). Tumor cells could destroy the basement membrane, penetrate the lower stroma, and grow outward in a crab-foot shape (13). Moreover, tumor cells tend to grow outward along existing blood vessels and integrate them as tumor expands (19). In addition to tumor angiogenesis, there are non-angiogenic mechanisms of vascular simulation such as vessel co-option and angiogenic mimicry (20,21). All of these factors may be the reasons for radial or penetrating vessels. Moreover, the same reasons explain the features of hyper-enhancement and earlier wash-in time. New tumor vessels are often formed as defective tumor endothelial cells and tumor pericytes with an irregular shape, high tortuosity, and low vasoreactivity, resulting in sluggish blood flow, which is performed as later wash-out time on CEUS (22). The bubble half-life is tens of minutes *in vivo*, and the time for contrast agent bubbles to start infusing breast tissue and fade varies from person to person (23). The characteristics of wash-in and wash-out time of lesions in this study were compared with those of the surrounding breast tissue to avoid the influence of contrast agent actuation duration.

CEUS combined with BI-RADS can improve the diagnostic efficiency for breast lesions. In this study, CEUS combined with BI-RADS showed a sensitivity of 84.8%, a specificity of 85.7% and an AUC value of 0.921. In the study conducted by Zhao *et al.* (24), CEUS combined with BI-RADS showed a sensitivity of 86.6%, a specificity of 96.8% and an AUC value of 0.917. Evaluation of blood vessels is helpful in differentiating between benign and malignant tumors. CEUS uses a 2.5-nanometer-sized microbubble and increases the contrast between microbubbles and background scattering through modern nonlinear imaging techniques so that the microcirculation in the lesion can be observed by the harmonic signal generated by the vibration of the microbubbles, and the detection ability of blood flow improved.

CEUS shows difference in diagnosis efficiency between lesions of different sizes. The overall model worked for lesions >1.0 cm (Groups 2 and 3), but was inefficient for lesions ≤1.0 cm (Group 1). It is inappropriate to use the same diagnostic model to diagnose lesions of different

sizes. A previous study by Li *et al.* (6) reported that for lesions with >2.0 cm size, CEUS showed differences in enhancement degree, margin, homogeneity, radial or penetrating vessels and scope, with a sensitivity of 87.7%, a specificity of 99.4%, and an AUC value of 0.812. Conversely, for lesions with ≤2.0 cm size, CEUS showed differences in all parameters except for heterogeneity and had a sensitivity of 70.8%, a specificity of 92.7%, and an AUC value of 0.778. However, their study distinguished lesions only by 2.0 cm, which was not sufficiently accurate and did not solve the problem of how to improve the diagnostic efficiency of small lesions.

To explore more suitable diagnostic models for lesions of different sizes, various diagnostic models were established. In Group 1, different parameters were included in M_1 to provide a new diagnostic criterion for lesions ≤1.0 cm. More features, such as earlier wash-in time and ill-defined margin, were added to M_1 than M_0, and blood perfusion defects and wash-out time were eliminated. As a result, the diagnostic efficiency of M_1 combined with BI-RADS has improved. Wan *et al.* (25) found that heterogeneous enhancement and perfusion defects were detected more frequently in large tumors (size, >2.0 cm) than in small tumors (size, ≤2.0 cm). It was explained by the phenomena that the inhomogeneous distribution of the vasculature system and internal necrosis tend to appear in large tumors. Buadu *et al.* (26) reported that MVD and uneven distribution play a major role in heterogeneous enhancement on CEUS. In addition, the larger the tumor size, the more likely it is to have an internal hypoxic environment, uneven distribution of vessels and internal necrosis with the tumor growth. Thus, different parameters need to be considered for small lesions, which is also the reason for the poor diagnostic efficacy of previous applications of CEUS for small lesions.

In Groups 2 and 3, although new models (M_2 and M_3) included different factors from the original model (M_0), diagnostic efficiency of M_2 and M_3 could not be significantly improved over that of M_0. Therefore, M_0 adapted perfectly for Groups 2 and 3, and there was no need to build different models to apply to breast lesions >1.0 cm.

This study has some limitations. First, this was a retrospective analysis, and only patients who underwent both US and CEUS were included, which could indicate a selection bias. Second, a quantitative analysis was not performed. Third, the influence of different pathological types on CEUS features was not evaluated. A multicenter prospective study is needed, and more data should be collected for further simplification and validation in the future.

Conclusions

In conclusion, the diagnostic performance of CEUS is closely related to lesion size. Establishing a new diagnostic model for lesions ≤1.0 cm can improve diagnostic performance of CEUS for breast lesions ≤1.0 cm.

Acknowledgments

Funding: This work was supported by the National Natural Science Foundation (grant number: 82071925).

Footnote

Reporting Checklist: The authors have completed the STARD reporting checklist. Available at https://gs.amegroups.com/article/view/10.21037/gs-23-223/rc

Data Sharing Statement: Available at https://gs.amegroups.com/article/view/10.21037/gs-23-223/dss

Peer Review File: Available at https://gs.amegroups.com/article/view/10.21037/gs-23-223/prf

Conflicts of Interest: All authors have completed the ICMJE uniform disclosure form (available at https://gs.amegroups.com/article/view/10.21037/gs-23-223/coif). The authors have no conflicts of interest to declare.

Ethical Statement: The authors are accountable for all aspects of the work in ensuring that questions related to the accuracy or integrity of any part of the work are appropriately investigated and resolved. This study was conducted in accordance with the Declaration of Helsinki (as revised in 2013). This study was a retrospective clinical diagnostic test, approved by the Ethics Committee of the Chinese PLA General Hospital (No. S2021-683-01). Informed consent was waived because of the retrospective nature of the study.

References

1. Chen C, Wang Y, Niu J, et al. Domain Knowledge Powered Deep Learning for Breast Cancer Diagnosis Based on Contrast-Enhanced Ultrasound Videos. IEEE Trans Med Imaging 2021;40:2439-51.
2. Liang X, Li Z, Zhang L, et al. Application of Contrast-Enhanced Ultrasound in the Differential Diagnosis of Different Molecular Subtypes of Breast Cancer. Ultrason Imaging 2020;42:261-70.
3. Li SY, Niu RL, Wang B, et al. Determining whether the diagnostic value of B-ultrasound combined with contrast-enhanced ultrasound and shear wave elastography in breast mass-like and non-mass-like lesions differs: a diagnostic test. Gland Surg 2023;12:282-96.
4. He H, Wu X, Jiang M, et al. Diagnostic accuracy of contrast-enhanced ultrasound synchronized with shear wave elastography in the differential diagnosis of benign and malignant breast lesions: a diagnostic test. Gland Surg 2023;12:54-66.
5. Chen Y, Tang L, Du Z, et al. Factors influencing the performance of a diagnostic model including contrast-enhanced ultrasound in 1023 breast lesions: comparison with histopathology. Ann Transl Med 2019;7:647.
6. Li C, Yao M, Shao S, et al. Diagnostic efficacy of contrast-enhanced ultrasound for breast lesions of different sizes: a comparative study with magnetic resonance imaging. Br J Radiol 2020;93:20190932.
7. Lagendijk M, van Maaren MC, Saadatmand S, et al. Breast conserving therapy and mastectomy revisited: Breast cancer-specific survival and the influence of prognostic factors in 129,692 patients. Int J Cancer 2018;142:165-75.
8. Mendelson EB, Böhm-Vélez M, Berg WA, et al. ACR BI-RADS® Ultrasound. In: ACR BI-RADS® Atlas, Breast Imaging Reporting and Data System. Reston, VA: American College of Radiology; 2013:35-75.
9. Wan C, Du J, Fang H, et al. Evaluation of breast lesions by contrast enhanced ultrasound: qualitative and quantitative analysis. Eur J Radiol 2012;81:e444-50.
10. Jia C, Niu Q, Liu L, et al. Value of an expanded range of lesions on contrast-enhanced ultrasound for the diagnosis of hypervascular breast masses. Gland Surg 2023;12:824-33.
11. Goubran HA, Kotb RR, Stakiw J, et al. Regulation of tumor growth and metastasis: the role of tumor microenvironment. Cancer Growth Metastasis 2014;7:9-18.
12. Grivennikov SI, Greten FR, Karin M. Immunity, inflammation, and cancer. Cell 2010;140:883-99.
13. Welch DR, Hurst DR. Defining the Hallmarks of Metastasis. Cancer Res 2019;79:3011-27.
14. Şener E, Şipal S, Gündoğdu C. Comparison of Microvessel Density with Prognostic Factors in Invasive Ductal Carcinomas of the Breast. Turk Patoloji Derg 2016;32:164-70.
15. Li YJ, Wen G, Wang Y, et al. Perfusion heterogeneity in breast tumors for assessment of angiogenesis. J Ultrasound Med 2013;32:1145-55.
16. Ternifi R, Wang Y, Polley EC, et al. Quantitative Biomarkers for Cancer Detection Using Contrast-Free Ultrasound High-Definition Microvessel Imaging: Fractal Dimension, Murray's Deviation, Bifurcation Angle & Spatial Vascularity Pattern. IEEE Trans Med Imaging 2021;40:3891-900.
17. Metz S, Daldrup-Unk HE, Richter T, et al. Detection and quantification of breast tumor necrosis with MR imaging: value of the necrosis-avid contrast agent Gadophrin-3. Acad Radiol 2003;10:484-90.
18. Uhlig J, Fischer U, Surov A, et al. Contrast-enhanced cone-beam breast-CT: Analysis of optimal acquisition time for discrimination of breast lesion malignancy. Eur J Radiol 2018;99:9-16.
19. Sander LM. Modeling contact guidance and invasion by cancer cells. Cancer Res 2014;74:4588-96.
20. Kuczynski EA, Vermeulen PB, Pezzella F, et al. Vessel co-option in cancer. Nat Rev Clin Oncol 2019;16:469-93.
21. Viallard C, Larrivée B. Tumor angiogenesis and vascular normalization: alternative therapeutic targets. Angiogenesis 2017;20:409-26.
22. Neeman M. Perspectives: MRI of angiogenesis. J Magn Reson 2018;292:99-105.
23. Albrecht T, Blomley M, Bolondi L, et al. Guidelines for the use of contrast agents in ultrasound. January 2004. Ultraschall Med 2004;25:249-56.
24. Zhao H, Xu R, Ouyang Q, et al. Contrast-enhanced ultrasound is helpful in the differentiation of malignant and benign breast lesions. Eur J Radiol 2010;73:288-93.
25. Wan CF, Du J, Fang H, et al. Enhancement patterns and parameters of breast cancers at contrast-enhanced

US: correlation with prognostic factors. Radiology 2012;262:450-9.
26. Buadu LD, Murakami J, Murayama S, et al. Breast lesions: correlation of contrast medium enhancement patterns on MR images with histopathologic findings and tumor angiogenesis. Radiology 1996;200:639-49.

Cite this article as: Fu N, Li J, Wang B, Jiang Y, Li S, Niu R, Wang Z. Diagnostic performance of contrast-enhanced ultrasound in breast lesions: what diagnostic models could be used for lesions of different sizes? Gland Surg 2023;12(12):1654-1667. doi: 10.21037/gs-23-223